

Palladium Nanoparticles-Decorated Graphene Nanosheets as Highly Regioselective Catalyst for Cyclotrimerization Reaction

Jinsheng Cheng^{1,2}, Longhua Tang², and Jinghong Li^{2,*}

¹Department of Chemistry, Chinese University of Science and Technology, Hefei 230026, China

²Department of Chemistry, Key Lab. of Bioorganic Phosphorus Chemistry and Chemical Biology, Tsinghua University, Beijing 100084, China

Novel palladium nanoparticles/graphene-based composites were prepared by a method involving palladium nanoparticles *in situ* growth on chitosan-functionalized graphene. The resulted composites showed uniform palladium nanoparticles distribution, which were characterized by Fourier transform infrared spectrometry (FTIR), transmission electron microscopy (TEM), scanning electron microscopy (SEM), Raman spectroscopy, atomic force microscopy (AFM), X-ray diffraction spectroscopy (XRD) and electron diffraction pattern (ED), etc. Moreover, such graphene-based nanocomposites were successfully applied to catalyze the cyclotrimerization of acetylene with high regioselectivity ($\geq 99.5\%$) and superior recycling performance without the assistance of any ligands.

Keywords: Graphene, Chitosan, Palladium, Composites, Catalyst.

Delivered by Publishing Technology to: York University
IP: 130.63.180.147 On: Wed, 13 Aug 2014 19:28:34
Copyright: American Scientific Publishers

1. INTRODUCTION

In recent years, graphene has attracted great interests due to the excellent mechanical, thermal and electronic properties arising from its unique sp^2 lattice structure of covalent carbon-carbon bonds.¹⁻⁴ Significantly, comparing with carbon nanotubes, this novel two-dimensional (2D) layered of sp^2 -bonded carbon possesses higher specific surface area,^{5,6} more extraordinary electronic transport properties and much more prominent wrinkles structure.^{7,8} Such fascinating properties render graphene as a promising candidate for metal nanoparticles (NPs) support. Recently, increasing research attention has been paid to various of NPs-graphene composites such as precious metal-graphene,^{9a-c} TiO₂-graphene,^{9d} CdS-graphene,^{9e} in which graphene served as efficient catalyst support used in direct methanol fuel cells, organic transformations, photocatalysis and photoelectrochemical cells, etc. Unfortunately, these graphene-based catalysts still have some shortcomings like limited efficient binding sites on the surfaces and nonuniform NPs distribution, which leading to the sharply decreased recycling efficiency (as Ref. [9b] stated, conversion for the fourth run declined sharply to 19%). Therefore, it is highly desirable to prepare high efficiency catalysts with more effective binding sites and surface

anchoring groups for metal cations on graphene oxide (GO) or graphene surfaces.

It's well known that chitosan is also widely used catalyst support owing to its chelating abilities with precious metals.¹⁰⁻¹¹ It was chosen to functionalize graphene nanosheets and then decorate with palladium NPs, which would combine both significant catalytic advantages of chitosan and graphene, such as low price, large surface area, good biocompatibility and high immobilization capacity for precious-metal catalysts.

Meanwhile, palladium-catalyzed coupling reactions have been a boon for organic synthesis over the past few decades. Reactions such as the Suzuki, Heck and Negishi are a few of the more notable carbon-carbon bond forming reactions which were awarded the Nobel Prize of 2010 in Chemistry. Another typical palladium-catalyzed coupling approach, highly regiocontrolled synthesis of arene via cyclotrimerization reaction, is also very important since arenes are key building blocks in organic and pharmaceutical synthesis.¹²⁻¹⁵ Most of the approaches are to employ helpful ligands coordinated with the precious metal catalyst, and then apply these complexes in the cyclotrimerization reactions of acetylenes. Nevertheless, besides the high costs of most ligands, high performance catalysts with good regioselectivity are still big challenges, especially for "electron-poor" acetylenes.^{12d, 13b, 16-18} Thus, in the past decades, how to improve the regiocontrol in the

*Author to whom correspondence should be addressed.

cyclotrimerization reactions of acetylenes is always in the face of the people of the world. Recent research efforts for such reactions have focused strongly on optimizing the regioselectivity of the reaction. Among various strategies, designing new catalysts by combining precious-metal NPs with an efficient support of choice instead of complicated ligands provides a broad scope for the discovery of novel, highly active and recyclable catalysts for industrially important cyclotrimerization transformations.^{13a}

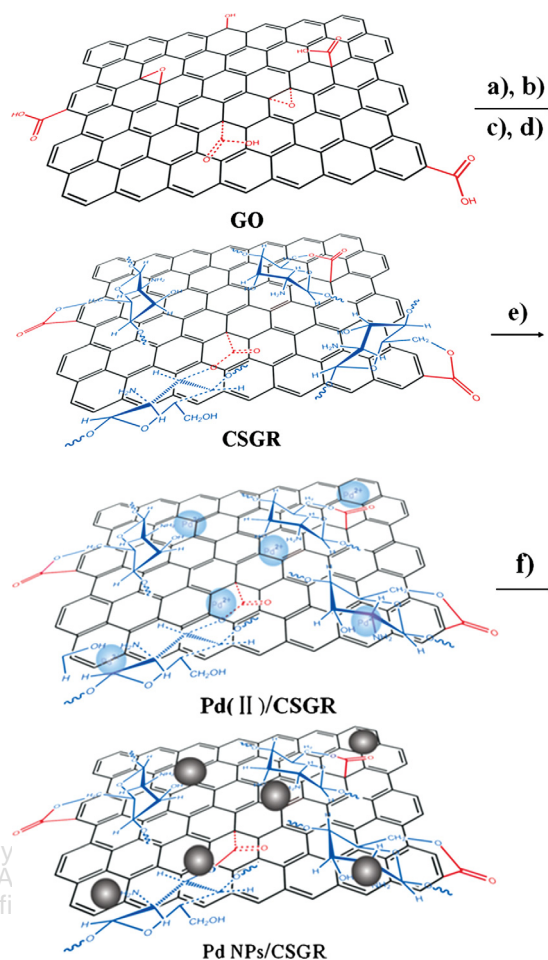
Herein, we report a facile preparation of Pd NPs/graphene composites through *in situ* growth of NPs on chitosan-functionalized graphene (Scheme 1). With the introduction of chitosan to the 2D layered graphene, the Pd NPs/chitosanfunctionalized graphene composites (Pd NPs/CSGR) exhibited near perfect catalytic conversion, regioselectivity behavior ($\geq 99.5\%$) and significantly enhanced recycling performance in cyclotrimerization reaction of acetylene without the assistance of any ligand.

2. EXPERIMENTAL DETAILS

2.1. Typical Synthetic Procedures for Chitosan Functionalized Graphene

GO was prepared as previous report.⁴ In this work, GO (200 mg) was dispersed in SOCl_2 (40 mL) together with DMF (1 mL), and then exfoliated by sonicating under ambient condition for 0.5 h. After refluxing for 52 h, the yellow-brown dispersion was converted to the acyl chloridebound graphene oxide (GO-COCl, 219.2 mg). Successively, dried phthaloyl chitosan (PHCS, 1.753 g, for the preparation method of phthaloyl chitosan, please see supporting information) and LiCl (1.201 g) were dispersed in dimethylacetamide (DMAC, 120 mL), and then stirred at 140 °C under dried nitrogen for 2 h.

After being cooled, GO-COCl (219.2 mg) was added followed by 14.0 mL of pyridine. The mixture was ultrasonicated for 1 h, then stirred, and refluxed under nitrogen for 48 h. Upon being cooled, the resultant mixture was filtered through a 0.22 μm pore size nylon membrane. A brown-coloured filtrate was collected and taken to dryness on a rotary evaporator. Followed by a complete removal of solvent, the resulting black solid was stirred in distilled water (120 mL) for 6 h. By filtration again, a black residue was collected on the 0.22 μm pore size nylon filter, accompanied with a red-brown aqueous solution. The residue was sonicated in water (200 mL) for 1 h, filtered, washed with another 1000 mL of deionized water, and then repeatedly extracted with water in a Soxhlet apparatus for 72 h. The final product was dried at 65 °C under vacuum for 24 h (weight of the PHCS-GO, 205 mg). Removal of the N-phthaloyl groups on PHCS-GO was carried out in below procedures: PHCS-GO (205 mg) was dispersed in hydration hydrazine (15 mL) at 80 °C for 16 h, after



Scheme 1. Schematic illustration of the preparation of Pd NPs/CSGR composites. Reaction conditions: (a) ClCH_2COOH , NaOH; (b) SOCl_2 , DMF, 70 °C; (c) Phthaloyl chitosan, LiCl, DMAC, N_2 , 130 °C; (d) Hydrazine hydrate, 16 h; (e) PdCl_2 , 24 h; (f) Ethylene glycol/ H_2O , pH 13, N_2 , 140 °C, 3 h.

reaction, the mixture was filtered and washed with deionized water for three times, finally, the product was dried at 65 °C under vacuum for 24 h (weight of the CSGR- NH_2 , 175 mg).

2.2. Typical Procedures for the Synthesis of Palladium NPs/Chitosan Functionalized Graphene Composites

Chitosan functionalized graphene (100 mg) was suspended in water (1.5 mL), subsequently, ethylene glycol (10 mL) was added. The mixture was then sonicated for 20 mins, palladium chloride ethylene glycol solution (10 mL 2.03 mg Pd/mL, prepared previously) was added dropwisely under stirred conditions.²⁷ Adjust the pH value of the system to 5–6, the mixture was then vigorously sonicated for 5 min and stirred overnight. In the next step, adjust the pH of the solution to above 13 with NaOH solution (2.5 M, in ethylene glycol), successively the solution

was heated at 140 °C for 3 h to ensure that Pd was completely reduced. The whole process was conducted under flowing N₂. After cooling to room temperature, the reaction mixture was filtered through a 0.2 μm PTFE membrane filter, washed intensively with deionized water and dried at 65 °C under vacuum for 24 h to give the Pd NPs/CSGR composites.

2.3. Catalytic Application of the Pd NPs/CSGR Composites in Cyclotrimerization Reaction

In a typical experiment, the Pd NPs/CSGR catalyst (100 mg) and trimethylchlorosilane (TMSCl, 2 mL) were dispersed in C₆H₆ (56.6 mL)/*n*-butanol (3.4 mL) mixed solvents with stirring at 40 °C, acetylene (10 mM) was then added to the above mixture dropwisely. After complete conversion of acetylenes as monitored by TLC, the reaction mixture was filtered through a 0.2 μm PTFE membrane filter. In this way, the catalyst was recovered and could be reused after sufficient washing together with vacuum-drying at 60 °C to remove organic impurities. The filtrate was carefully collected and the solvents were removed by rotary evaporation to give crude products, then further purified by preparative TLC on silica gel (eluent: light petroleum ether-ethyl ether etc.). The conversions were measured by GC analysis using an internal standard.

3. RESULTS AND DISCUSSION

3.1. Catalyst Design and Preparation

In this work, the starting material GO was prepared as previous report.⁴ Then the exfoliated GO sample was activated with chloroacetic acid in order to convert any hydroxyl groups to carboxylic acid groups (the intermediate was named GO-COOH), which increased its solubility in water, and made more carboxylic acid groups available for subsequent chitosan functionalization.

Chitosan is also widely used as the catalyst support owing to its low price and large surface area etc. Besides, the presence of amine functional groups in chitosan gives it interesting chelating properties for metal cations, thus introduces more binding sites and surface anchoring groups for precious-metal catalysts. Currently, there are two potential mechanisms for the adsorption of precious-metal ions onto chitosan surface. One involves the four amino (–NH₂) groups on chitosan chains serving as coordination sites that interact with metal ions. Another possibility is that two amino (–NH₂) groups and two hydroxyl (–OH) groups coordinate with precious-metal ions.^{17b, 17c} Successful surface functionalization of graphene with chitosan can combine catalytic advantageous properties of both graphene and chitosan, and introduce more effective binding sites and surface anchoring

groups on the graphene surface, which is very important for an effective catalyst. To synthesize the supported Pd NPs catalysts, a yellow-brown dispersion of GO-COOH was mixed with SOCl₂ and DMF, then this mixture was refluxed for 52 h while stirring. The resultant product GO-COCl was added to a dispersion of phthaloyl chitosan (PHCS, see supporting information) and LiCl in DMAC, which was then refluxed under nitrogen for 48 h. Successively, through deprotection of the *N*-phthaloyl protecting groups with hydrazine hydrate, the intermediate CSGR (chitosan/graphene) was obtained. Pd NPs/CSGR (Pd NPs chitosan/graphene) composites were readily formed after treating the mixed dispersion of CSGR and palladium chloride with ethylene glycol. The presence of amine functional groups in CSGR leads to chelating effects with metal cations, thus providing more effective binding sites and surface anchoring groups for precious-metal NPs in comparison with raw graphene.^{19, 20} In addition, Pd (II) ions can also be captured by any remaining carboxylic anions in CSGR through coordination effects. In a successive step, by simple reduction with ethylene glycol, Pd NPs can be deposited onto the catalyst support, and any remaining oxygen-containing groups in the CSGR intermediate can be further reduced simultaneously.

During above processes, the abundant carboxylic acid groups in GO-COOH can provide active sites for the reactions with hydroxyl or amine groups in chitosan, forming ester or amide linkages, respectively. Thus through formation of these linkages, chitosan can be grafted onto GO readily.

3.2. Characterization of the Composites

The AFM image in Figure 1(a) shows that the GR nanosheets are mostly single layered (height~0.81 nm) and 200–800 nm in lateral width. Previous work has also assigned a similar 0.8 nm thickness for graphene single layered structures.²¹ Figure 1(b) shows that the height of the CSGR structure (about 200–1000 nm in lateral width) as measured from the depth profile analysis was about 2.07 nm, which could be considered as a single-layered graphene nanosheet covalently grafted to a single-layered chitosan nanosheet, indicating the successful functionalization of chitosan to graphene nanosheets.

Figures 2(a–b) show the TEM images of graphene and CSGR nanosheets, respectively, clearly illustrating the nearly transparent flake-like shapes with characteristic crumpled silk waves. The TEM image of Pd NPs/CSGR is shown in Figure 2(c). It is easy to see that the graphene nanosheets were decorated randomly and uniformly by the nanosized Pd particles, and few particles were free from the supports, indicating a strong interaction between the particles and supports. The Pd NPs are in the size range of 2–9 nm (with the majority of particles formed being

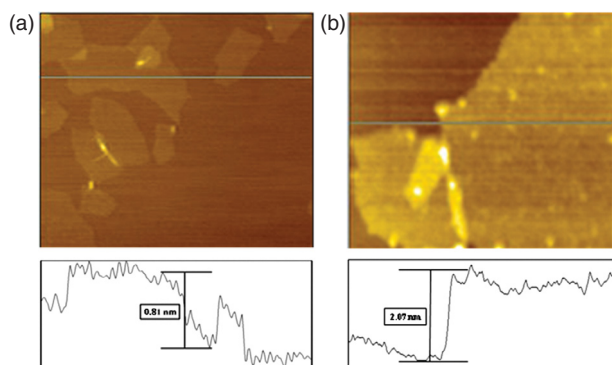


Fig. 1. (a) AFM image and depth profile of graphene on mica substrate, size $2.0 \times 2.0 \mu\text{m}$; (b) AFM image and depth profile of CSGR, size $1.0 \times 1.0 \mu\text{m}$.

about 4–5 nm in diameter, Fig. 2(d)). The TEM images in Figure S3 show the isolated catalyst Pd NPs/CSGR-NH₂ after two catalytic recycles, confirming the maintained presence of crystalline Pd(0) (see supporting information). The above results reveal that the present method can produce stable and small sized Pd NPs. HRTEM image in Figure 2(f) taken of the surface of Pd NPs/CSGR shows that the Pd NPs have a polycrystalline structure. The arrows in Figure 2(f) show the lattice spacing is 0.223 nm, similar to the Pd (111) lattice spacing. The electron

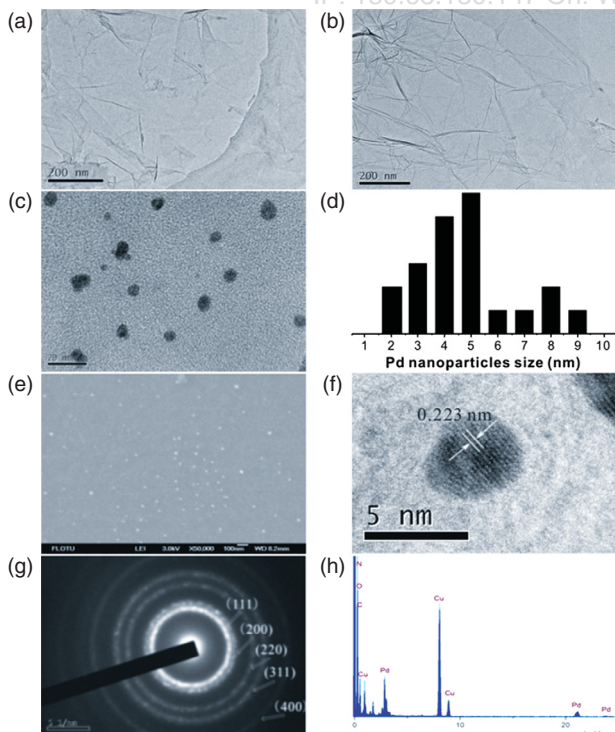


Fig. 2. TEM images of (a) raw graphene; (b) CSGR; (c) Pd NPs/CSGR catalyst and (d) histogram showing the size distribution of the Pd NPs; (e) SEM image of Pd NPs catalysts; (f) HRTEM image of Pd NPs/CSGR catalyst and (g) ED of Pd NPs/CSGR; (h) Energy-dispersive X-ray analysis of Pd NPs/CSGR composites.

diffraction pattern (ED) shown in Figure 2(g) indicates the Pd NPs supported on CSGR have a uniform and narrow particle size distribution, which is also confirmed by the SEM images in Figure 2(e). The polycrystalline nature of Pd NPs produces four X-ray diffraction rings in sequence from inner to outer can be indexed to the (111), (200), (220), and (311) of the face-centered cubic Pd panes, respectively (Fig. 2(g)). An energy-dispersive X-ray analysis taken from a random assembly Pd NPs/CSGR also identifies the Pd nature supported on CSGR (Fig. 2(h)).

As shown in Figure 3, the Raman spectra of CSGR and Pd NPs/GR display two prominent peaks at 1590 and 1331 cm^{-1} , which correspond to the well-documented G and D bands of graphene. XRD patterns in Figure 4(a) reveal that CSGR nanosheets have a peak at $2\theta = 24.7^\circ$, the same characteristic peak as graphene,²² further confirming the structure of the graphene based CSGR. The most representative reflections of Pd(0) are indexed as face-centered cubic (fcc) with unit cell parameter $a = 0.39026 \text{ nm}$. The Bragg reflections at 39.6° , 45.5° and 67.3° correspond to the indexed planes of the crystals of Pd(0) (111), (200), (220). The strongest peak at 39.6° demonstrates that the (111) Pd(0) crystal face is the exclusive effective crystal face which catalyzes $[2 + 2 + 2]$ cyclotrimerization reaction.²³

FTIR spectra reveal the successful attachment of chitosan to graphene. FTIR spectra of CSGR presented in Figure 5 and Figure S2 show two bands of the glucopyranose rings, appearing at approximately 890 and 1150 cm^{-1} , respectively, indicating the existence of the chitosan. And the characteristic peak of graphene is 1545 cm^{-1} (attributed to skeletal vibrations of graphene), which could be observed on curves a–e in Figure 5, implying the successfully combination of the chitosan to graphene.

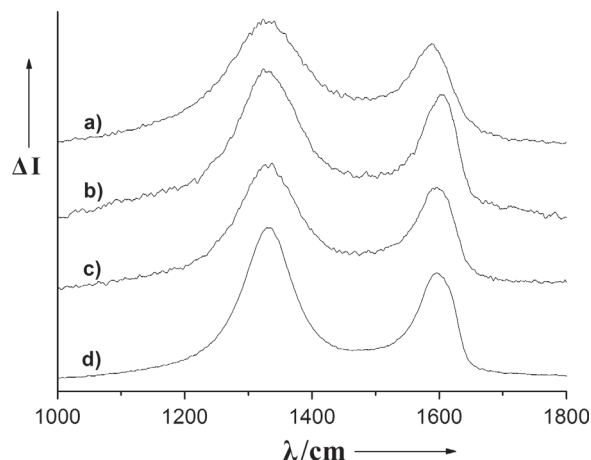


Fig. 3. Raman spectroscopy of (a) graphene; (b) CSGR-OH; (c) CSGR-NH₂ and (d) Pd NPs/GR.

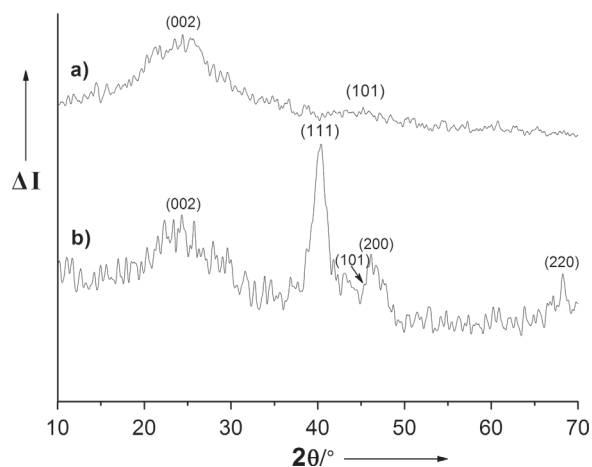


Fig. 4. XRD patterns of (a) CSGR and (b) Pd NPs/CSGR.

3.3. Catalytic Application of Pd NPs/CSGR Composites in Cyclotrimerization Reaction

We investigated the catalytic performance of Pd NPs/CSGR composites. A summary of the results for Pd NPs/CSGR catalyzed cyclotrimerization of acetylenes is listed in Table I. We first used graphene as the catalyst support. The cyclotrimerization reaction of methyl propiolate (**1a**) was examined in the presence of 3 mol% Pd NPs/GR catalyst. Investigations revealed that the reaction proceeded smoothly in benzene/*n*-butanol (10:0.6, v/v) at 40 °C for 8 h in the presence of TMSCl, affording two products **2a** and **3a** in a 90.56:9.44 ratio (72.4% yield, entry 2, Table S1).

Above results show that regioselectivity was still a big challenge. Thus, as an improved strategy, we chose CSGR instead of bare unmodified graphene as the catalyst support. Experiments showed that the reaction afforded much better control of regioselectivity in the presence of Pd NPs/CSGR-NH₂ (100:0, 96.5% yield, entry 4, Table S1)

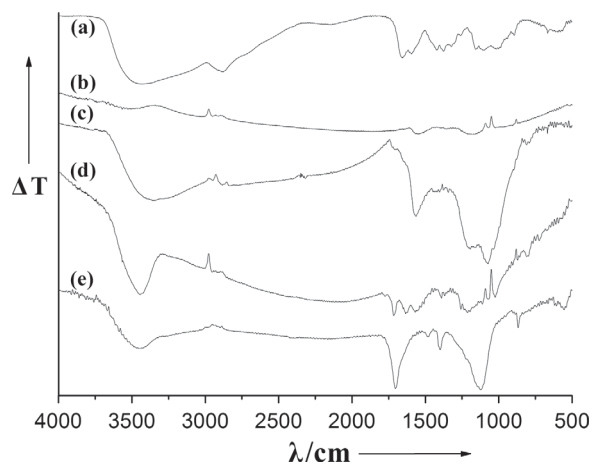
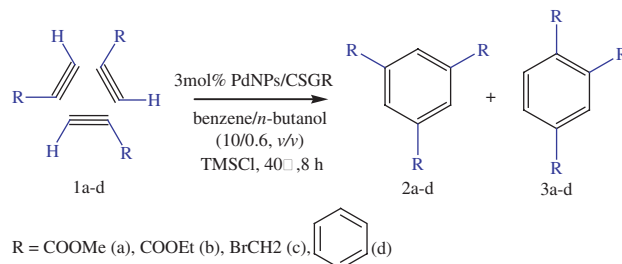


Fig. 5. FTIR spectra of (a) chitosan; (b) graphene; (c) chitosan functionalized graphene (CSGR-OH); (d) chitosan functionalized graphene (CSGR-NH₂) and (e) Pd NPs supported on CSGR-OH.



Scheme 2. Pd NPs/CSGR composites catalyzed cyclotrimerization reaction of acetylene.

comparing with unmodified graphene based catalyst, indicating that the grafting of chitosan to graphene surface was much beneficial in producing regiocontrolled **2a**.

Encouraged by these results, in order to find the optimum catalyst, a series of cyclotrimerization reactions of **1a** catalyzed by different Pd NPs/CSGR composites with variable structures were carried out. Briefly, the Pd NPs/CSGR-NH₂ composites (marked Cat. 1, bearing –NH₂ terminal groups, instead of –OH groups stretching outwards the composites surfaces), Pd NPs/CSGR-OH (marked Cat. 2, possesses abundant –OH terminal groups, instead of –NH₂ groups), and Pd NPs/ECSGR-NH₂ (marked Cat. 3, holds –NH₂ terminal groups, for the preparation of ECS, please see supporting information). Experimental results show that the variable structures of CSGR in these composites could affect the catalytic performance obviously. For example, catalysis by Cat. 1 and Cat. 3, the reactions proceed with higher yields (96.5%, 96.9%, respectively) and better regioselectivity (both 100%) (entries 4–5, Table S1), showing a better catalytic efficiency than that of Cat. 2 (89.3%, regioselectivity 99.50:0.35, entry 3, Table S1), indicating that when the terminal groups of the composites are –NH₂ groups (thus holds more binding sites for metal ions), the composites will exhibit superior catalytic performance than the catalyst with –OH terminal groups.

Why Pd NPs/CSGR catalysts have such superior performance for regioselective cyclotrimerization reaction? Firstly, we proposed that the CSGR nanosheets provide a relatively large surface area and high immobilization capacity on which to deposit highly active catalytic Pd NPs, which is very helpful for catalytic efficiency. Secondly, the Pd NPs generated *in situ* by mild ethylene glycol reduction can form smaller spherical Pd NPs (a median

Table I. Recycling experiment with Pd NPs/CSGR-NH₂ catalyst.^a

Run	Isolated yields (%)
1	96.5
2	93.8
3	91.2
4	87.4
5	70.7

^aFormation of Trimethyl-1, 3, 5-tricarboxylate.

size distribution of 4–5 nm) dispersed uniformly over the few-layered CSGR support, size being another important factor for high catalytic performance (as a comparison, commercially available Pd/C, which contained 28–34 μm palladium particles, showed much lower yield as well as a sharply lowered regioselectivity in this reaction, entry 1, Table I). Thirdly, after grafting spatial conformational chitosan to the graphene surface, the strong steric repulsion between CSGR nanosheets could prevent the NPs on the same nanosheet or different nanosheets from fusing together during the reaction, explaining why Pd NPs/CSGR catalysts showed better recycling performance than Pd NPs directly on GO or graphene. Meanwhile, the presence of conformational chitosan on CSGR induces the cyclotrimerization reaction to form 1, 3, 5-isomers (possessing less steric hindrance) prior to 1, 2, 4-isomers.

Finally, the recyclability of the catalyst was studied. Pd NPs/CSGR-NH₂ (Cat. 1) catalyzed [2+2+2] cyclotrimerization of **1a** was chosen as the model reaction. Experimental results show that the catalytic activity dropped successively in the second, third and fourth runs of the reaction (93.8%, 91.2%, 87.4%, respectively, entries 2–4, Table I), with a yield of 70.7% for the fifth run (entry 5, Table I). All these results are obvious higher than previous report,^{9b} in which the conversion for the fourth run declined to 19% despite showing 100% conversion in the first run.

4. CONCLUSION

In conclusion, we demonstrated an effective way to synthesize the Pd NPs/CSGR composites by *in situ* growth of Pd NPs on chitosan-functionalized graphene. This novel covalent surface modification of graphene with chitosan can combine both the significant advantages of chitosan and graphene. The composites were applied successfully in the cyclotrimerization reaction of acetylenes with high regio-control ($\geq 99.5\%$). Their exceptionally high activities and good recycling performance make them attractive low-cost alternatives to commercially available Pd catalysts such as Pd/C.

SUPPORTING INFORMATION

S1. MATERIALS AND CHARACTERIZATION

S1.1. Materials

Graphite powder (99.99995%, 325 mesh), PdCl₂ and palladium on activated carbon (Pd/C) powder (5%) were purchased from Alfa Aesar. Graphene and graphene oxide were synthesized by modification of a reported procedure. Chitosan was supplied by National Medicine Group, Shanghai, China (the degree of deacetylation was 90%,

and the molecular weight was 125 000 g·mol⁻¹. The chitosan was ground and sieved, and the 0–125 μm fraction was used for experiments), all solvents and other reagents were purchased from Beijing Chemicals Co. Ltd. as analytical-grade products.

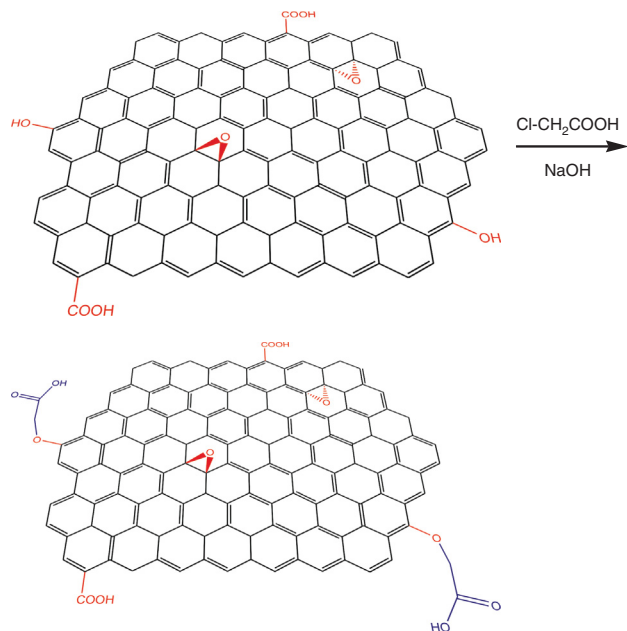
S1.2. Characterization

The powder X-ray diffraction (XRD) measurements of the samples were recorded on a Bruker D8 Advance X-ray powder diffraction meter using Cu K α radiation ($\lambda = 1.5406 \text{ \AA}$) with scattering angles (2θ) of 8–60°. JEOL JEM 1200EX and JEOL JEM 2010 transition electronic microscopy were used for transmission electron microscopy (TEM) analysis and high-resolution transmission electron microscopy (HRTEM, equipped with energy dispersive X-ray spectroscopy (EDS, Oxford) and selected area electron diffraction (SAED)) analysis, respectively. Samples were prepared by placing one drop of an ethanol suspension of the Pd NPs/CSGR hybrid material onto a copper grid (3 mm, 200 mesh) coated with carbon film. A JSM-7401 scanning electron microscopy (SEM) operated at 20 kV was used to analyze the sample. Raman spectroscopy (Renishaw microprobe RM1000) was recorded at a wavelength of 633 nm (He-Ne laser). Atomic force microscopic (AFM) images were taken out using a Nanoscope III Multi Mode SPM (Digital Instruments) with an AS-12 (“E”) scanner operated in tapping mode in conjunction with a V shaped tapping tip (Applied Nanostructures SPM model: ACTA). The images were taken at a scan rate of 2 Hz. Fourier transform infrared (FTIR) spectra were carried out on a Spectrum One (Perkin Elmer) spectrometer from KBr pellets. The Element analysis was performed with CE-440 (EAI Co., USA). Isomer ratios of the products were analyzed on a GC-MS Spectrometer in EI mode using Perkin Elmer ASXL/MS Turbomass instrument, the product partition was done on PE-5 capillary column (30 m \times 0.25 mm \times 0.25 μm), oven temperature programmed from 50 °C–210 °C at 5 °C/min with an initial hold of 2 mins. All ¹H NMR and ¹³C NMR spectra were recorded at 600 MHz using CDCl₃ or d₆-DMSO as solvent using JEOL JNM-ECA 600 spectrometer (¹H NMR at 600 MHz and ¹³C NMR at 150 MHz). TLC (thin layer chromatography) was performed using commercially prepared 100–400 mesh silica gel plates (HF₂₅₄, Qingdao Haiyang Chemical Co. Ltd.), and visualization was effected at 254 nm. All melting points are uncorrected.

S2. PREPARATION OF GRAPHENE, GO-COOH AND CHITOSAN FUNCTIONALIZED GRAPHENE

S2.1. Preparation of Graphene

Graphite oxide was prepared by modified Hummers method. ¹Preparation of graphene was carried out by



Scheme S1. Illustrations of the preparation procedures for GO-COOH.

adding hydrazine hydrate (0.5 mL) into the dispersion of graphene oxide (50 mg) powder in water (50 mL) after sonicating for 1 h, and the mixture was stirred for 24 h at 50 °C. Finally, black hydrophobic powder graphene was obtained by filtrating the product and drying in vacuum.

S2.2. Preparation of GO-COOH

The obtained GO (200 mg) was suspended in deionized water (100 mL) to give a concentration of ~ 2 mg/mL, and then sonicated for 1 h to give a clear solution. NaOH (12.0 g) and chloroacetic acid (ClCH_2COOH , 10.0 g) were then added to the GO suspension and sonicated for another 2 h to convert the $-\text{OH}$ groups to COOH , giving GO-COOH.^{2,3} The resulting GO-COOH solution was neutralized, and purified by repeated rinsing and filtrations. Finally, the product was dried in vacuum for 24 h at 60 °C.

S2.3. Preparation of Chitosan Functionalized Graphene

S2.3.1. Preparation of Phthaloyl Chitosan (PHCS)

Chitosan (0.300 g, 1.86 mmol pyranose) was added to a solution of 0.83 g (5.6 mmol) of phthalic anhydride in 6 mL of *N,N*-dimethylformamide (DMF) containing 5% water (*v/v*), and the mixture was heated in nitrogen at 120 °C with stirring. After 8 h reaction, the resulting pale tan mixture was cooled to room temperature and poured into ice water. The precipitate was collected on a filter, washed with 150 mL of methanol at room temperature for 1 h, and dried to give the product (0.448 g) as a pale tan powdery material.

S2.3.2. Preparation of Epichlorohydrin-Crosslinked Chitosan (ECS)

A solution of 0.010 M epichlorohydrin containing 0.067 M sodium hydroxide was prepared (pH 10). Freshly prepared wet chitosan beads were added to this epichlorohydrin solution to obtain a ratio of 1:1 with chitosan. The chitosan beads in epichlorohydrin were heated to a temperature between 40 and 50 °C for 2 h and stirred continuously. Then the beads were filtered and washed intensively with distilled water to remove any unreacted epichlorohydrin and air dried. The newly formed cross-linked chitosan (ECS) beads were ground to a constant size (250 μm) before use.

S2.3.3. Preparation of Chitosan Functionalized Graphene (CSGR-NH₂)

The obtained GO-COOH (200 mg) was dispersed in SOCl_2 (40 mL) together with DMF (1 mL), exfoliation was carried out by sonicating the above mixture under ambient condition for 0.5 h. Then the resulting homogeneous yellow-brown dispersion was refluxed for 52 h to convert the graphene oxide-bound carboxylic acids into acyl chlorides (final weight of GO-COCl, 219.2 mg). In a typical experiment, carefully dried PHCS (1.753 g) and LiCl (1.201 g) were dispersed in DMAC (dimethyl acetamide, 120 mL), heated to 130 °C, and stirred under dried nitrogen for 2 h. After being cooled, GO-COCl (219.2 mg) was added followed by addition of pyridine (14.0 mL). The mixture was sonicated for 1 h, and refluxed under nitrogen for 48 h with stirring. Upon being cooled, the resultant mixture was filtered through a 0.22 μm pore size PTFE membrane. A brown-coloured filtrate was collected and taken to dryness on a rotary evaporator. Followed by a complete removal of solvent, the resulting black solid was stirred in deionized water (120 mL) for 6 h, by filtration again, a black residue was collected on the 0.22 μm pore size nylon filter, accompanied with a red-brown aqueous solution. The residue was sonicated in water (200 mL) for 1 h, filtered, washed with another batch of deionized water (1000 mL) of water, and then repeatedly extracted with water in a Soxhlet apparatus for 72 h. The intermediate product (PHCS/GO) was dried at 65 °C under vacuum for 24 h (weight of the PHCS/GO, 205 mg).

Deprotection of the *N*-phthaloyl groups on PHCS/GO was carried out according to the following procedures: PHCS/GO (205 mg) was dispersed in hydration hydrazine (15 mL) at 80 °C for 16 h, after reaction, the mixture was filtered and washed with deionized water for three times. Finally, the intermediate was dried at 65 °C under vacuum for 24 h (weight of the CSGR-NH₂, 175 mg). In this step, most of the epoxy groups and other oxygen-bearing groups on the graphene oxide surface were also reduced.

Table S1. Catalytic performances comparisons for commercial 5% Pd/C, Pd NPs/GR and Pd NPs/CSGR catalysts.^a

Entry	Catalyst	Acetylene	Conversion ^b	Yield ^c (%)	Regioselectivity ^d
1	5%Pd/C ^e	1a	35.1	18.7	76.16:23.84 ^f
2	Pd NPs/GR	1a	79.2	72.4	90.56:9.44
3	Pd NPs/CSGR-OH	1a	97.6	89.3	99.50:0.35 ^g
4	Pd NPs/CSGR-NH ₂	1a	100	96.5	100:0
5	Pd NPs/ECSGR-NH ₂	1a	100	96.9	100:0
6	Pd NPs/CSGR-NH ₂	1b	100	99.1	100:0
7	Pd NPs/CSGR-NH ₂	1c	100	98.5	100:0 ^h
8	Pd NPs/CSGR-NH ₂	1d	100	97.8	100:0 ⁱ

^aThe reaction conditions were as follows: acetylene (10 mM), catalyst (3 mol %). TMSCl (2 mL) in benzene/*n*-butanol (60 mL, 10:0.6, *v/v*) at 40 °C for 8 h. ^bDetermined by GC analysis. ^cIsolated yield. ^dRatio of 1, 3, 5-isomer and 1, 2, 4-isomer, detected by GCMS. ^eThe diameter of the Pd particles was 28–34 μm. ^fSome unidentified brown oil was also isolated. ^gSome unidentified compounds were also detected (0.15%). ^hThe reaction was at 80 °C under argon for 16 h, some unidentified oil was also observed. ⁱ20 h was needed instead of 8 h.

S2.3.4. Preparation of Chitosan Functionalized Graphene (CSGR-OH)

A stock solution of chitosan in aqueous acetic acid was prepared by dissolving 2 g chitosan in 200 mL of aqueous acetic acid. Grafting of chitosan onto the graphene surface was conducted by using EDC (1-ethyl-3-(3-dimethylaminopropyl) carbodiimide and NHS (N-hydroxysuccinimide) as coupling agents, in which GO were dispersed in deionized water followed by reaction with a mixture of EDC and NHS (EDC/NHS = 1:2.5) for 2 h to activate the carboxylic acid groups on the graphene oxide. Subsequently, the desired amount of chitosan solution was added into the GO dispersion with vigorous stirring. Then the mixture was carried out at 88 °C for 24 h under N₂. After reaction, the reaction mixture was centrifuged, and washed with ethanol and distilled water for several times, the obtained brown black solid was collected and dried at 65 °C under vacuum for 24 h, the intermediate was called CSGR-OH. In this step, most of the epoxy groups and other oxygen-bearing groups on the graphene oxide surface were also reduced.

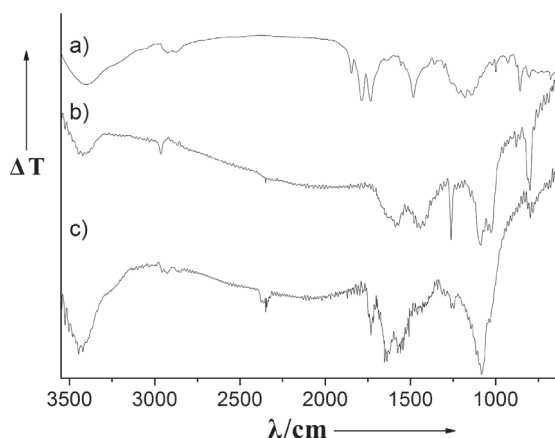


Fig. S2. FTIR spectra of (a) phthaloyl chitosan; (b) ECSGR and (c) Pd NPs/ECSGR.

S3. CATALYTIC PERFORMANCE OF THE PD NPs/CSGR COMPOSITES

Experimental results revealed that in addition to **1a**, other acetylenes with different functional groups such as esters (ethyl propiolate, **1b**), bromines (3-bromo-1-propyne, **1c**), and aromatic rings (phenylacetylene, **1d**, tested as a reference) groups are tolerated. Catalyzed by Pd NPs/CSGR-NH₂ (Cat. 1), the reactions of **1b**, **1c** and **1d** proceeded smoothly with yields of 99.1%, 98.5%, 97.8%, respectively, all exclusively producing 1, 3, 5-isomers (entries 6–8, Table S1), indicating that the catalysts can provide superior regiocontrol in the cyclotrimerization reaction.

S4. CHARACTERIZATION OF PD NPs/CSGR CATALYST

S5. PROOFS FOR THE CYCLOTRIMERIZATION PRODUCTS

Trimethyl-1, 3, 5-tricarboxylate (2a) Solid, mp 145–148 °C. ¹H NMR (600 MHz, CDCl₃, 27 °C): δ 3.9854 (s, 9H), 8.8480 (s, 3H); ¹³C NMR (150 MHz, CDCl₃, 27 °C): δ 52.6623, 76.8961, 77.1067, 77.3174, 131.2712, 134.6224, 165.4435; MS *m/z*: 253, 252, 222, 221, 193, 147, 102, 75; IR (KBr, cm⁻¹): 3093, 3022, 2964, 2847, 1725, 1435, 1260, 1002, 873, 744, 718, 493.

Trimethyl-1, 2, 4-tricarboxylate (3a) Solid, mp 38–40 °C. ¹H NMR (600 MHz, CDCl₃, 27 °C): δ 3.8804 (s, 3H), 3.8953 (s, 3H), 3.9148 (s, 3H), 7.6918–7.7158 (s, 1H), 8.1367–8.1464 (d, 1H), 8.3537–8.3777 (d, 11H); ¹³C NMR (150 MHz, CDCl₃, 27 °C): δ 52.8443, 52.9113, 76.9440, 77.1546, 77.3652, 128.9158, 130.2658, 131.6638, 132.2670, 132.4872, 165.3382, 166.8223, 167.5691; MS *m/z*: 253, 252, 222, 221, 193, 103, 75, 59; IR (KBr, cm⁻¹): 3009, 2951, 2899, 2847, 1731, 1435, 1299, 1241, 1112, 1067, 989, 860, 751, 577, 493.

Triethyl-1, 3, 5-tricarboxylate (2b) Solid, mp 134–140 °C. ¹H NMR (600 MHz, CDCl₃, 27 °C): 1.4338–1.4579 (m, 9H), 4.4469–4.4710 (m, 6H), 8.8411 (s, 3H); ¹³C NMR (150 MHz, CDCl₃, 27 °C): δ 14.3346, 61.7105, 76.9152, 77.1259, 77.3461, 131.5106, 134.4213,

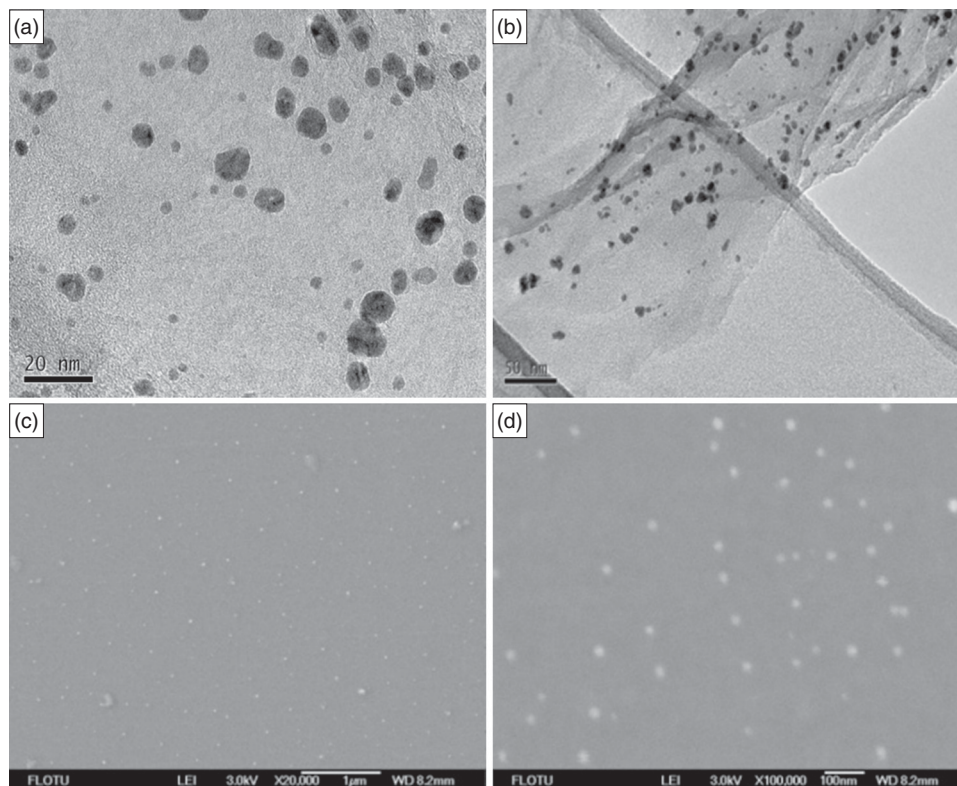


Fig. S3. Typical images of the recycled catalyst (Pd NPs/CSGR-NH₂) after 2 run of reactions. (a–b) TEM images, and (c–d) SEM images.

165.0510; MS m/z : 296, 294, 249, 221, 193, 148, 88, 75, 73, 65; IR (KBr, cm⁻¹): 3093, 2996, 2944, 2906, 2880, 1725, 1441, 1389, 1241, 1099, 1022, 938, 731, 486.

1, 3, 5-Tris(bromomethyl) benzene (2c) Solid, mp 94–100 °C. ¹H NMR (600 MHz, CDCl₃, 27 °C): δ 4.4526 (s, 6H), 7.3524 (s, 3H); ¹³C NMR (150 MHz, CDCl₃, 27 °C): δ 32.2394, 76.8769, 77.0876, 77.3078, 129.6435, 139.1512; MS m/z : 360.86, 355.89, 349.57, 315.36, 279.97, 278.94, 276.94, 274.89, 207.25, 198.99,

195.97, 118.05, 117.04, 115.01, 102.01, 91.03, 89.03, 60.00, 57.94, 57.30, 51.00; IR (KBr, cm⁻¹): 3020, 2972, 1803, 1601, 1456, 1423, 1213, 1117, 891, 851, 706, 584, 560.

1, 3, 5-Triphenyl benzene (2d) Solid, mp 173–175 °C. ¹H NMR (600 MHz, CDCl₃, 27 °C): δ 7.4730–7.4845 (m, 3H), 7.5520–7.5772 (m, 6H), 7.7868–7.7994 (m, 6H), 7.8864 (s, 3H); ¹³C NMR (150 MHz, CDCl₃, 27 °C): δ 77.0014, 77.2216, 77.4323, 125.3636, 127.5466, 127.7285, 129.0307, 141.3534, 142.5407; MS m/z : 308, 307, 306, 289, 228, 153, 132, 77; IR (KBr, cm⁻¹): 3060, 3028, 2899, 1590, 1486, 1409, 1080, 1022, 880, 751, 699, 609, 506.

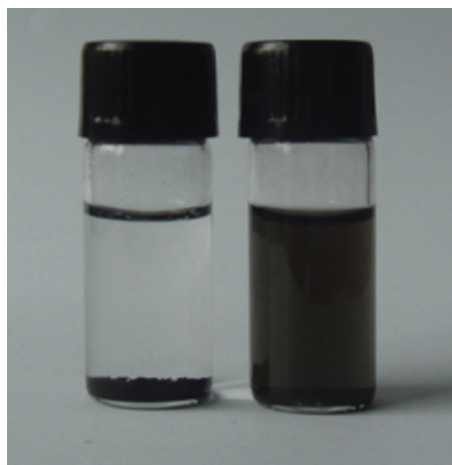


Fig. S4. Photos of the samples dispersion (1 mg/mL) 30 minutes after ultrasonication: graphene in water (left) and Pd NPs CSGR-NH₂ in 5% HAc (right).

Acknowledgments: We thank National Natural Science Foundation of China (No. 11079002) and National Basic Research Program of China (No. 2007CB310500, No. 2011CB935700) for financial support.

References and Notes

- (a) A. K. Geim, *Science* 324, 1530 (2009); (b) S. J. Park and R. S. Ruoff, *Nat. Nanotechnol.* 4, 217 (2009); (c) A. K. Geim and K. S. Novoselov, *Nat. Mater.* 6, 183 (2007).
- (a) D. V. Kosynkin, A. L. Higginbo-Tham, A. Sinitkii, J. R. Lomeda, A. Dimiev, B. K. Price, and J. M. Tour, *Nature* 458, 872 (2009); (b) P. Sutter, *Nat. Mater.* 8, 171 (2009).
- (a) N. M. R. Peres, *J. Phys.: Condens. Matter.* 21, 323201 (2009); (b) S. R. Wang, M. Tambraparni, J. J. Qiu, J. Tipton, and D. Dean,

- Macromolecules* 42, 5251 (2009); (c) S. J. Park, D. A. Dikin, S. B. T. Nguyen, and R. S. Ruoff, *J. Phys. Chem. C* 113, 15801 (2009).
4. (a) J. L. Xia, F. Chen, J. H. Li, and N. J. Tao, *Nat. Nanotechnol.* 4, 505 (2009); (b) L. H. Tang, Y. Wang, Y. M. Li, H. B. Feng, J. Lu, and J. H. Li, *Adv. Funct. Mater.* 19, 2782 (2009); (c) F. Chen, Q. Qing, J. Xia, J. H. Li, and N. J. Tao, *J. Am. Chem. Soc.* 131, 9908 (2009); (d) W. S. Hummers and R. E. Offeman, *J. Am. Chem. Soc.* 80, 1339 (1958).
 5. M. J. McAllister, J. L. Li, D. H. Adamson, H. C. Schniepp, A. A. Abdala, J. Liu, M. Herrera-Alonso, D. L. Milius, R. Car, R. K. Prud'homme, and I. A. Aksay, *Chem. Mater.* 19, 4396 (2007).
 6. B. Z. Jang and A. Zhamu, *J. Mater. Sci.* 43, 5092 (2008).
 7. A. K. Geim and K. S. Novoselov, *Nat. Mater.* 6, 183 (2007).
 8. (a) A. H. Castro Neto, F. Guinea, N. M. R. Peres, K. S. Novoselov, and A. K. Geim, *Rev. Mod. Phys.* 81, 109 (2009); (b) F. Chen and N. J. Tao, *Acc. Chem. Res.* 42, 429 (2009); (c) S. J. Park and R. S. Ruoff, *Nat. Nanotechnol.* 4, 217 (2009); (d) M. J. Allen, V. C. Tung, and R. B. Kaner, *Chem. Rev.* 110, 132 (2010).
 9. (a) Y. M. Li, L. H. Tang, and J. H. Li, *Electrochem. Commun.* 11, 846 (2009); (b) G. M. Scheuermann, L. Rumi, P. Steurer, W. Bannwarth, and R. Mülhaupt, *J. Am. Chem. Soc.* 131, 8262 (2009); (c) C. Xu, X. Wang, and J. W. Zhu, *J. Phys. Chem. C* 112, 19841 (2008); (d) H. Zhang, X. J. Lv, Y. M. Li, Y. Wang, and J. H. Li, *ACS Nano* 4, 380 (2010); (e) H. X. Chang, L. H. Tang, and J. H. Li, *Electrochem. Commun.* 12, 483 (2010).
 10. (a) T. Vincent and E. Guibal, *Ind. Eng. Chem. Res.* 41, 5158 (2002); (b) D. J. Macquarrie and J. J. E. Hardy, *Ind. Eng. Chem. Res.* 44, 8499 (2005).
 11. Y. C. Cui, L. Zhang, and Y. Li, *Polym. Adv. Technol.* 16, 633 (2005).
 12. (a) D. W. Goodman, *Nature* 454, 948 (2008); (b) K. Tanaka, *Asian J. Chem.* 4, 508 (2009); (c) B. Heller and M. Hapke, *Chem. Soc. Rev.* 36, 1085 (2007); (d) S. Saito and Y. Yamamoto, *Chem. Rev.* 100, 2901 (2000); (e) S. Kotha, E. Brahmachary, and K. Lahiri, *Eur. J. Org. Chem.* 22, 4741 (2005).
 13. (a) Y. Y. Lin, S. C. Tsai, and S. J. Yu, *J. Org. Chem.* 73, 4920 (2008); (b) A. Geny, N. Agenet, L. Iannazzo, M. Malacria, C. Aubert, and V. Gandon, *Angew. Chem. Int. Ed.* 48, 1810 (2009); (c) N. Agenet, V. Gandon, K. P. C. Vollhardt, M. Malacria, C. Aubert, *J. Am. Chem. Soc.* 129, 8860 (2007).
 14. (a) B. R. Galan, T. Rovis, *Angew. Chem. Int. Ed.* 48, 16, 2830 (2009); (b) B. M. Trost, *Science* 254, 1471 (1991).
 15. (a) J. Varela and C. Saá, *J. Organomet. Chem.* 694, 143 (2009); (b) R. Sanz, *Org. Prep. Proc. Int.* 40, 215 (2008); (c) B. Heller and M. Hapke, *Chem. Soc. Rev.* 36, 1085 (2007); (d) S. Saito and Y. Yamamoto, *Chem. Rev.* 100, 2901 (2000).
 16. V. Cadierno, S. E. García-Garrido, and J. Gimeno, *J. Am. Chem. Soc.* 128, 15094 (2006).
 17. J. M. Renga, A. G. Olivero, and M. Bosse, Patent Number. 4959488 (1990).
 18. G. C. Jia, S. I. D. Williams, S. Y. Herman, and P. Xue, *J. Organomet. Chem.* 691, 1945 (2006).
 19. E. Guibal, *Sep. Purif. Technol.* 38, 43 (2004).
 20. C. Mack, B. Wilhelmi, J. R. Duncan, and J. E. Burgess, *Biotech. Adv.* 25, 264 (2007).
 21. X. Li, X. Wang, L. Zhang, S. Lee, and H. J. Dai, *Science* 319, 1229 (2008).
 22. Y. Wang, Y. M. Li, L. H. Tang, J. Lu, and J. H. Li, *Electrochem. Commun.* 11, 889 (2009).
 23. D. Stacchiola, H. Molero, and W. T. Tysoc, *Cat. Today* 65, 3 (2001).
 24. J. L. Gardea-Torresdey, J. G. Parsons, E. J. Gomez Peralta-Videa, H. E. Troiani, P. Santiago, and M. J. Yacaman, *Nano Lett.* 2, 397 (2002).
 25. A. K. Jhingan and W. F. Maier, *J. Org. Chem.* 52, 1161 (1987).
 26. X. M. Sun, Z. L., K. W., J. T. Robinson, A. G. S. Zaric, and H. J. Dai, *Nano Res.* 1, 203 (2008).
 27. W. Z. Li, C. H. Liang, W. J. Zhou, J. S. Qiu, G. Q. Sun, and Q. Xin, *J. Phys. Chem. B* 107, 6292 (2003).
 28. S. K. Mukerji and L. Singh, *Nature* 150, 347 (1942).
 29. A. Hebeish, A. Higazy, and A. El-Shafei, *Starch* 58, 401 (2006).
 30. O. V. Sibikina, A. A. Iozep, and B. V. Passet, *Russ. J. Appl. Chem.* 77, 263 (2004).

Received: 15 October 2010. Accepted: 13 December 2010.